Materials Science in Semiconductor Processing 72 (2017) 99–105

Contents lists available at ScienceDirect

Materials Science in Semiconductor Processing

journal homepage: www.elsevier.com/locate/mssp

Structural phase-dependent resistivity of intrinsic-extrinsic co-doped transparent titanium dioxide films

Kashif Safeen[a,b,c,*], V. Micheli[b], R. Bartali[b,c], G. Gottardi[b], Akif Safeen[a,d], Hafeez Ullah[b,c], E. Iacob[b], M. Fidrizzi[b], N. Laidani[b]

[a] Abdul Wali Khan University, Department of Physics, 23200 Mardan, Pakistan
[b] Center for Materials and Microsystems, Fondazione Bruno Kessler, Via Sommarive 18, 38123 Povo, Trento, Italy
[c] University of Trento, Department of Physics, Via Sommarive 15, 38123 Povo, Trento, Italy
[d] Department of Physics, Balochistan University of Information Technology, Engineering & Management Science (BUITEMS), Quetta, Pakistan

ARTICLE INFO

Keywords:
Transparent conducting oxides
TiO_2 thin films
RF sputtering
Structure properties
Electrical properties
Optical properties

ABSTRACT

The authors report a method of enhancing the conductivity of TiO_2 films by controlling their structural phases. Thin films of Nb:TiO_2 (TNO) were prepared on glass and silicon substrates by RF sputtering with varying Nb content at 200 °C. It is shown that fine control over the structural phases of TiO_2 is critical for achieving low resistivity. The resistivity values of the films doped with oxygen vacancies and Nb^{+5} decreased from 3.8×10^{-1} to $4.1 \times 10^{-3}\ \Omega$ cm when the weight percent of rutile in anatase-rutile phase mixture decreases from 52.8% to 32%. Furthermore, the lowest resistivity value of $2.37 \times 10^{-3}\ \Omega$ cm was obtained for the doped TiO_2 films having single phase anatase structure. The physical processes responsible for the diverse electrical properties are discussed and are associated with the growth conditions. Our result indicates that highly conductive doped-TiO_2 film can be obtained by controlling the anatase phase formation via the growth temperature. The obtained results can significantly contribute to the development of transparent electrodes by RF sputtering, a suitable technique for coating large area substrates.

1. Introduction

Transparent conducting oxides (TCOs) have wide-ranging applications in devices such as liquid crystal displays, photovoltaics, architectural and window glass technologies [1]. The performance of such devices is strongly correlated with the desired key properties such as structural phases, electrical resistivity, transparency and optical band gap. Currently, much effort is devoted to explore alternative oxide-based transparent conductors to fulfill the fast growing demand in many optoelectronic devices (flat panel display, photovoltaics etc). Among the TCOs, doped titanium dioxide is a promising material for such applications due its low-cost, excellent chemical stability especially in a reducing atmosphere and high transmittance in the infrared region, beside its excellent conductivity and transparency [2,3]. Therefore, in the recent years, interest in doped TiO_2 films has increased considerably due to the above mentioned useful properties and the potential applications as transparent electrodes.

The conductivity of TiO_2 films is strongly correlated with their crystalline structure particularly with the amount of anatase phase with respect to rutile and with the oxygen vacancies present in the film [4,5]. To grow anatase phase of TiO_2, thin films are usually grown in Ar-O_2 discharges because oxygen rich film inhibit anatase to rutile transformation and enhance the transparency of the films [5,6]. However, for low energetic conditions such as low power density (1 W/cm^2), high sputtering pressure (> 1.3 Pa) etc., growth in Ar-O_2 discharges is not favorable for oxygen vacancies creation owing to the spontaneous formation of oxygen interstitials in oxygen-rich deposition conditions [7]. Oxygen interstitials are predicted to be detrimental defects for the electrical properties of the film as they removes not only the oxygen vacancies but also form localized shallow acceptor states which compensates the electrons-doping by Nb^{+5} ions thus depressing the conductivity [8,9]. On the other hand, in the defective samples (oxygen deficient films), oxygen vacancies accelerate the atomic diffusion by providing a low energy mass transport route and promote the crystallization of thermodynamically stable rutile phase, which is undesirable for electrical properties of TiO_2 [6]. An attempt to stabilize the oxygen-deficient anatase phase in thin film of TiO_2 was made by growing them on single crystalline $SrTiO_3$ (STO) and $LiAlO_3$ (LAO) substrates because their lattice constant (a ~ 3.79 Å) is comparable to the in-plane lattice constant of anatase TiO_2 (3.78 Å) [2,10]. The low lattice mismatch

* Corresponding author at: Abdul Wali Khan University, Department of Physics, 23200 Mardan, Pakistan.
E-mail address: kashifsafeen@awkum.edu.pk (K. Safeen).

http://dx.doi.org/10.1016/j.mssp.2017.09.037
Received 3 May 2017; Received in revised form 5 September 2017; Accepted 28 September 2017
Available online 05 October 2017
1369-8001/

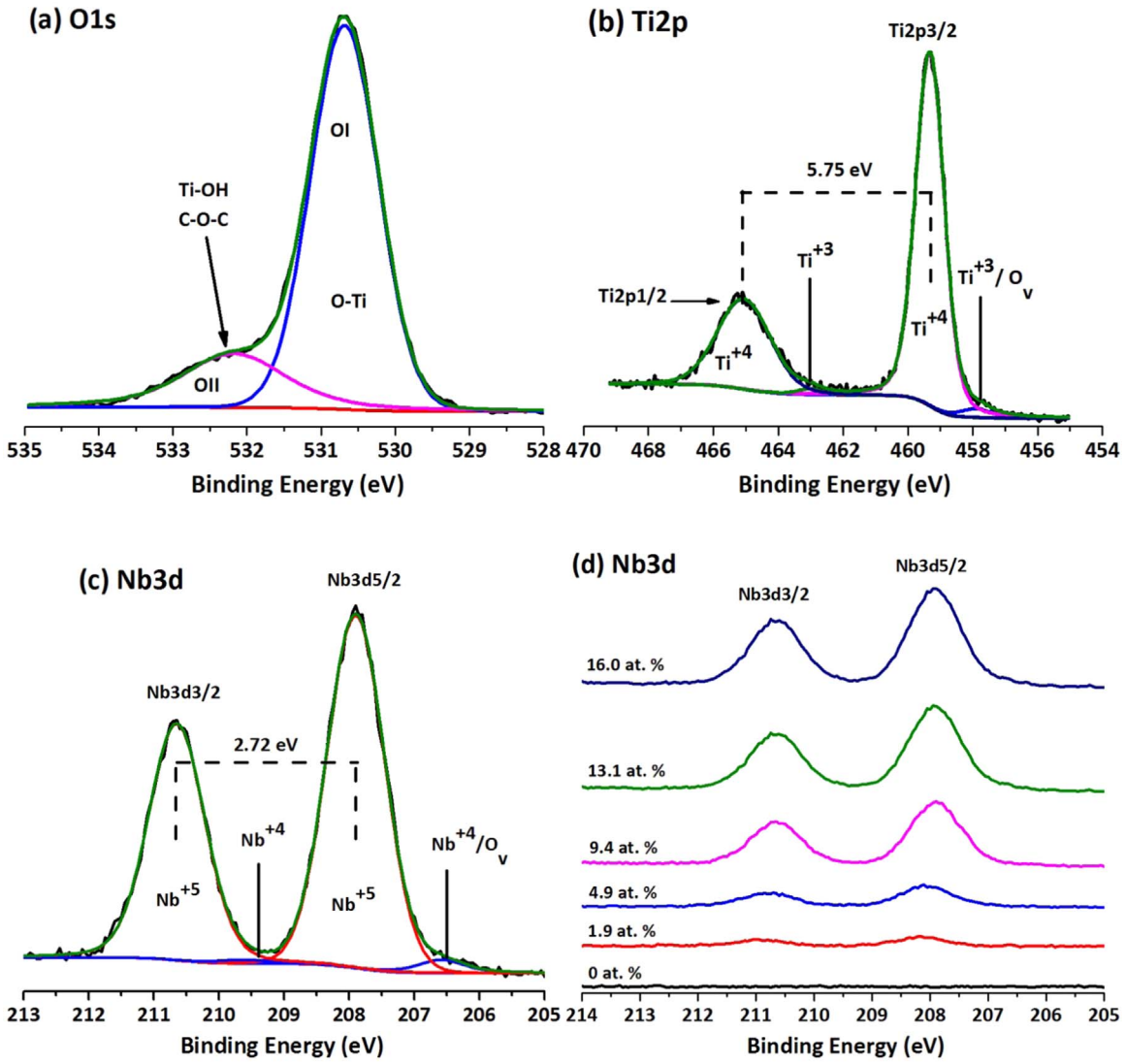

Fig. 1. (a) XPS O1s spectrum of the Nb:TiO_2 films (b) XPS Ti2p core-level spectrum (c) XPS Nb3d core-level spectrum of the as-grown TNO film deposited at 200 °C (d) Nb core-level with increasing Nb concentrations.

between anatase TiO_2 and STO/LAO substrates assisted the preferential growth of highly-oriented anatase TiO_2 film, which is the most suitable phase for transparent conducting properties [10]. Unfortunately, STO and LAO substrates are expensive, hence not really viable for industrial application. In fact under a practical point of view, TCOs film should be preferably deposited over glass or plastic substrates to minimize the cost of the final product. It is therefore crucial finding a feasible way to grow thermodynamically metastable anatase phase TiO_2 film on an economical substrates (glass and polyimide) with high conductivity.

In this work, we present a method to control the various structural phases of TiO_2 that critically influences its electrical properties. The deposition temperature was the experimental parameter whose optimization was used to stabilize the defective anatase phase instead of growing anatase structure in oxygen-rich condition or of using high-cost LAO/STO substrates. We obtained a lowest resistivity of the order of 10^{-3} Ω cm for single anatase structure whereas mixed anatase-rutile phase leads to highly resistive films. Based on the X-ray diffraction results, the electrical properties of the doped TiO_2 films were correlated with the growth temperature parameter.

2. Materials and methods

Nb:TiO_2 films were grown by radio frequency co-sputtering (13.56 MHz) in Ar plasma. An optimized ceramic TiO_2 (99.9% purity), 10 cm of diameter, produced by Materion and Nb_2O_5 (99.95% purity) 5 cm diameter, produced by ACI Alloys was used as sputtering targets. The films were grown on p-type silicon (100) and corning glass substrates at room temperature and at 200 °C. The total pressure of the growth chamber was fixed at an optimal value of 1.33 Pa [5,11]. The power applied to the Nb_2O_5 target was varied from 4 to 12 W (bias voltage: 59–110 V) while the power applied to the TiO_2 target was kept fixed at 78 W (RF self-bias voltage ~ −850 V). Different Nb concentrations in the films (1.9–16.0 at%) were obtained by changing the power applied to the target. The thicknesses of the films were in the range 125–170 nm. The as-deposited films were subsequently annealed in pure argon gas (pressure = 1.33 Pa) at 400 °C for 1 h. The detailed experimental procedure can be found in [6,11,12]. It is important to note here that in this article, primarily the results obtained from the films deposited at 200 °C and annealed at 400 °C is presented while the results of the films grown at room temperature and annealed at 350 °C is mentioned for reference.

The discharge properties were studied using Optical Emission Spectroscopy (OES) where the plasma light (in the wavelength range 200–850 nm with a spectral resolution of 0.2 nm) was collected with an optical fiber through a quartz window of the sputtering chamber. Subsequently, the light was analyzed by means of a Spectrapro 2300i

instrument, equipped with an ICCD camera. A surface profiler (Tencor Instruments) was used to measure the film thicknesses. Structural phases of the deposited films were obtained from X-ray diffraction analysis (Italstructures APD2000) using grazing angle configuration (0.3°). The atomic force microscopy (AFM) images were acquired with a Solver Px Scanning Probe Microscope from NT-MDT. AFM data were acquired in semi-contact mode with a silicon tip (~10 N/m, ~232 kHz) with a nominal radius of less than 10 nm. Analyses were performed on different scanning areas, 10 × 10 mm^2 and 5 × 5 mm^2. The surface morphology of the prepared sample is also analyzed with Scanning electron microscope (Jeol JSM-7401F). The chemical properties of the prepared films were investigated using X-ray photoelectron spectroscopy. A Scienta ESCA 200 spectrometer with a monochromatic Al Kα X-ray source (1486.6 eV) was employed to acquire the C1s, O1s, Ti2p and Nb3d core lines (resolution of 0.4 eV at 150 eV pass energy). The spectra deconvolution was made using a homemade software based on R platform [13]. The electrical properties, including resistivity, carrier concentration and carrier mobility, were characterized by van der Pauw and Hall Effect measurement (RH 2030 PhysTech) at room temperature. Optical transmittance of the deposited films was measured by a UV–VIS–NIR spectrophotometer (Model–JASCO V-670) in a wavelength range 200–2800 nm.

3. Results and discussion

3.1. Films chemical properties

The chemical properties of Nb:TiO_2 films are reported in detail elsewhere [5,6]. Briefly, the O1s XPS spectrum comprises of two peaks located at a binding energy (BE) of 530.41 and 532.13 eV (Fig. 1(a)). The lower BE peak (referred as OI) can be ascribed to oxygen bound to Ti^{+4} and Nb^{+5} in Nb:TiO_2 whereas the higher BE component located at 532.13 eV may arise due to the oxygen involvement in the Ti–OH bonds and possibly C–O–C, C–OH groups [14,15]. The $Ti2p_{3/2}$ and $Ti2p_{1/2}$ components of Ti2p core-level peak are positioned at 459.35 eV and 465.11 eV, respectively indicating that Ti is present in +4 valence states (Fig. 1(b)). Further, the $Ti2p_{3/2}$ peak has a clear shoulder located at 457.99 eV which is due to oxygen vacancies in the film as explained in our work [6,11]. We observed that the Ti^{+3}/Ti^{+4} atomic ratios increased from 0.007 to 0.088 when the power applied at the Nb_2O_5 target was increased from 4 to 12 W. The increase in the Ti^{+3}/Ti^{+4} atomic ratios (or density of oxygen vacancies) may be ascribed to the rise in Ar^+ ratio concentrations in the plasma with increasing power (see Table 1 for details). Ar^+ ions are in fact one of the most energetic species in Ar discharges [6,11]. From Fig. 1(c), we can observe that the $Nb3d_{5/2}$ and $Nb3d_{3/2}$ peaks are located at 207.90 eV and 210.65 eV, respectively, which means that the peaks originate from Nb^{+5} state. A low-intensity shoulder peak located at 206.44 indicates also the presence of +4 oxidation state of niobium (NbO_2). Further as shown in Fig. 1(d)) and Table 1, the niobium concentration in the films increased from 1.9 to 16.0 at% when the applied power was changed from 4 to 12 W.

Table 1
Ar^+/Ar emission intensity ratio, Nb concentrations obtained from XPS (at%), Ti^{+3}/Ti^{+4} atomic ratios, binding energy (BE) values of O_I, Ti2p, Nb3d core-lines of the as-deposited TiO_2 films grown at different powers applied to Nb_2O_5 target.

Power (W)	$(Ar^+/Ar)_{OES}$	Nb at%	$(Ti^{+3}/Ti^{+4})_{XPS}$	BE (O_I) (eV)	BE ($Ti^{+4}2p3/2$) (eV)	BE ($Nb^{+5}2d5/2$) (eV)
0	1.61	0	0.006	530.87	459.61	Not detected
4	1.71	1.9	0.007	530.91	459.68	208.15
6	1.74	4.9	0.021	530.88	459.60	208.06
8	1.79	9.4	0.033	530.81	459.35	207.90
10	1.81	13.1	0.072	530.85	459.35	207.97
12	1.88	16.0	0.088	530.87	459.34	207.99

3.2. Films structural and morphological properties

The surface morphology and microstructure of the most conductive Nb-doped TiO_2 film (resistivity ~ 2.37 × 10^{-3} Ω cm) was characterized by scanning electron microscope (SEM) and atomic force microscope (AFM) and is illustrated in Fig. 2(a) and (b). The SEM micrograph indicated well-adhered, dense and crack-free Nb:TiO_2 films over a wide area. The SEM micrograph also shows that the obtained film exhibited a smooth, uniform, and flat texture. Further, the AFM image for the surface morphologies of Nb-doped TiO_2 thin film is shown in Fig. 2(b). The prepared film has surface roughness around 0.58 nm and root mean square roughness of 0.76 nm. Such a small root mean square roughness suggests that Nb-doped TiO_2 films grown on silicon substrate have smooth surfaces. This type of surface roughness is common for sputter-deposited nanocrystalline TCO films of similar thickness [16].

The XRD profile of the as-deposited un-doped and Nb-doped TiO_2 films prepared at 200 °C is shown in Fig. 3(a). The peak at 27.46° which corresponds to (110) diffraction plane confirms the formation of nanocrystalline rutile phase for TiO_2 films. In contrast, Nb:TiO_2 films consisted of mixed phases of anatase and rutile for Nb concentrations ≤ 4.9 at% and amorphous structure for Nb content ≥ 9.4 at%. The films grown at 200 °C were subsequently annealed at 400 °C in pure argon gas (pressure = 1.33 Pa) in order to activate the dopants in TiO_2 lattice. For the annealed samples, we observed that the initial phase/structure of the TNO films determines the final structure after thermal annealing (see Fig. 3(b)). For TiO_2 films, the diffraction peak at 27.44° confirmed the formation of single phase rutile structure. For Nb:TiO_2 films with Nb ~ 1.9 and 4.9 at%, the (101) and (110) diffraction peaks at 25.20° and 27.38° indicate the growth of anatase and rutile mixed phases. The relative weight fractions of rutile phase in the anatase-rutile phases mixture was estimated using the relation [17]:

$$R(\%) = \left(\frac{I_R}{0.886 I_A + I_R}\right) \times 100 \quad (1)$$

In Eq. (1) I_R and I_A is the intensity of the most intense rutile and anatase peak ((110) and (101) in this case) and 0.886 is a unit-less correction factor to account for the differences in scattering intensities due to the different crystal structures. The rutile phase proportion in TNO films were around 52.80% and 32% for TNO films doped with 1.9 and 4.9 at% Nb respectively (Fig. 4(a)). For Nb concentrations in the range 9.4–13.1 at%, the as-grown amorphous films transformed to anatase structure with (101), (103), (004) and (200) crystallographic planes at the diffraction angles 25.08, 37.38, 38.3 and 48.2°. For the highest Nb content (16.0 at%), again mixed phases of anatase and rutile were detected in XRD (anatase: 65%, rutile: 35%). It is generally accepted that the total ion flux impinging onto the substrates and its energy drive the crystallization of the films. For TiO_2 film doped with 16.0 at% Nb, the concentration of Ar^+ ions available in the discharge which can bombard the surface of the growing films was found by OES higher (Ar^+/Ar = 1.88) compared to that measured during the deposition of films doped with 9.4 and 13.1 at% Nb (≤ 1.81). These energetic plasma conditions create more oxygen vacancies in the heavily doped films as can be inferred from the high Ti^{+3}/Ti^{+4} atomic ratio (~ 0.09), which was deduced from the XPS. During the annealing treatment, the Ti-O-Ti network weakens and the oxygen vacancies facilitate the Ti-O bond breaking and a consequent structural rearrangement to a thermally more stable rutile phase [18]. Further, the crystallites size of anatase as estimated by Scherrer equation [19] was around 27 ± 2 nm which is larger than previously reported by Ishida et al. for 450 °C annealed Nb:TiO_2 films, 20 nm [20].

As discussed above, the TNO films grown at 200 °C and subsequently annealed at 400 °C have mixed anatase-rutile structure for most of the Nb contents. The mechanism of the rutile phase formation may

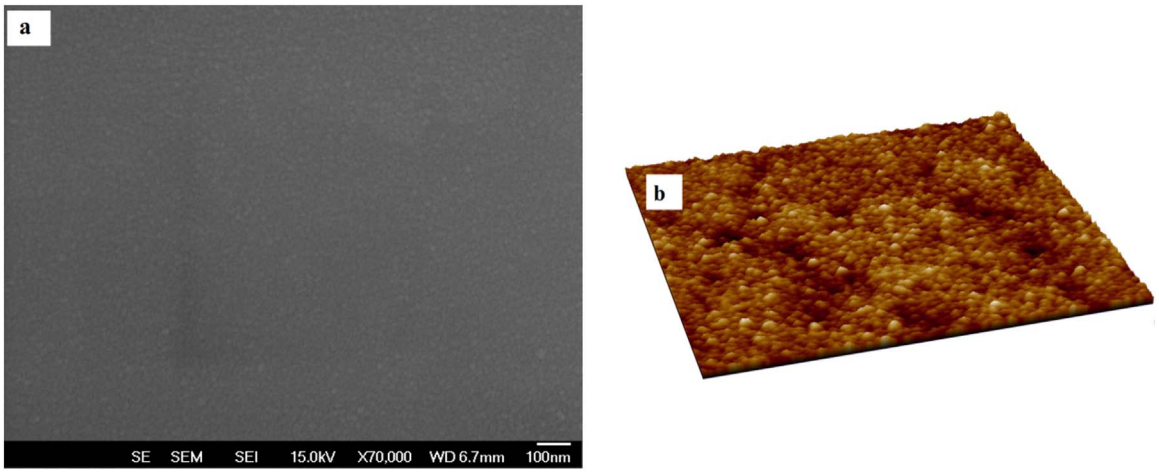

Fig. 2. (a) SEM micrographs of the conductive Nb-doped TiO_2 films annealed at 400 °C (b) Representative AFM topographic scan of the conductive Nb-doped TiO_2 sample annealed at 400 °C. Each topographic scan is 10×10 mm^2.

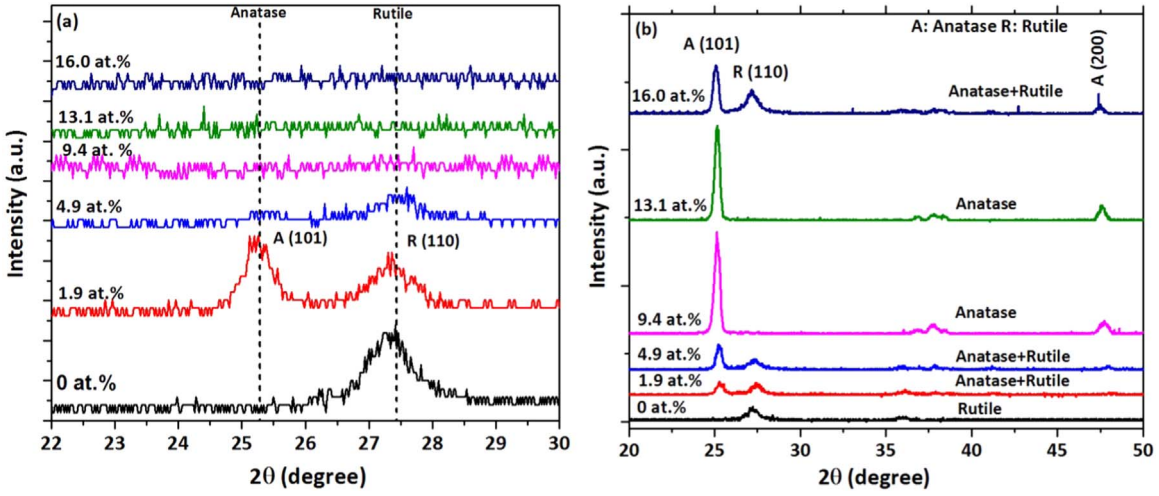

Fig. 3. XRD spectra of the TNO films for different Nb amount (a) as-grown TNO films deposited at 200 °C (b) TNO films annealed in argon at 400 °C. "R" and "A" denotes rutile and anatase phase in the XRD spectra.

be as following. When the substrate is heated to a growth temperature of 200 °C, the surface condition of the substrate is likely to be more energetic compared to the cold substrate. Further, energy for the diffusion of adatoms may also supplied by the plasma species which create oxygen vacancies and this energy can lower the activation energy for the formation of crystalline rutile phase [21]. As a result, the

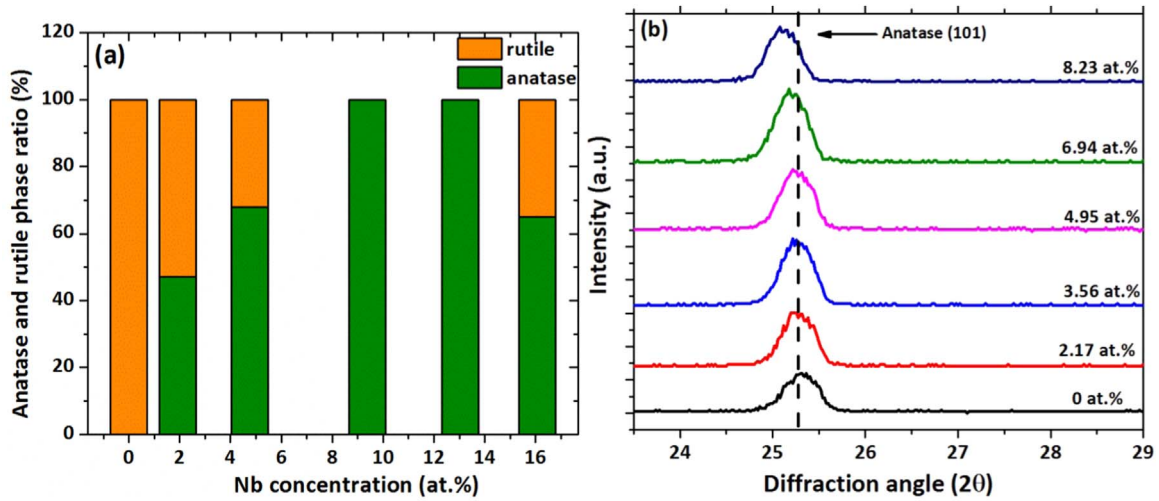

Fig. 4. (a) Anatase and rutile phase weight ratio of the TNO samples annealed at 400 °C for different Nb concentrations (b) XRD spectra of the TNO films deposited at room temperature and annealed at 350 °C.

surface diffusion during the films growth on the hot substrate allows for the development of thermodynamically stable rutile phase.

As reported in our work [5], oxygen vacancies are crucial for the conductivity of oxides. On the other hand, the rutile phase is detrimental: its formation was therefore controlled by adjusting the substrate temperature, without compromising the formation of oxygen vacancies. In other words, the formation of rutile phase was restricted by depositing the films at room temperature. On a cold substrate, the sputtered particles do not have sufficient energy and hence the adatoms do not have adequate mobility to overcome the potential energy barrier for a crystalline phase and therefore are frozen in an amorphous state [6]. Therefore, we propose the effective and cost-efficient route of using the growth temperature parameter to induce the formation of defective anatase phase (and obtain low resistive films) instead of growing the material in oxygen-rich plasma or using high cost LAO and STO substrates to stabilize the anatase phase. Exploring this route, we deposited Nb:TiO_2 films (Nb 0–8.23 at%) at room temperature and subsequently we annealed them at 350 °C (see Fig. 4(b)). The obtained structures were single phase defective anatase exhibiting resistivities in the range $10^{-3}-10^{-4}$ Ω cm.

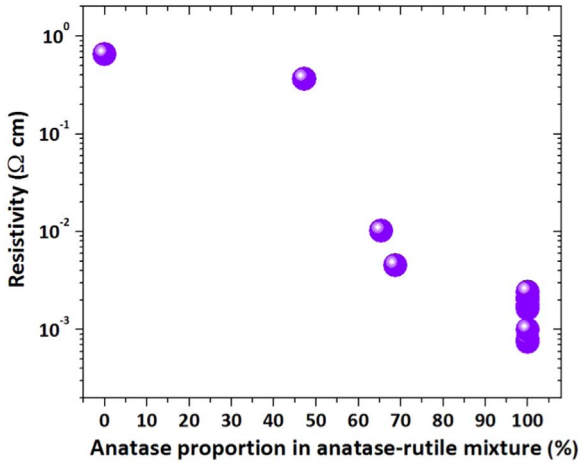

Fig. 5. Correlation between resistivity and phase proportion of anatase in anatase-rutile mixture in the annealed TNO films obtained at room temperature and 200 °C. The digit "0%" indicates pure rutile structure while "100%" represents single anatase phase in the film.

3.3. Electrical properties of Nb:TiO_2 films

The as-deposited Nb:TiO_2 films grown at 200 °C on glass were semiconducting (ρ ~ 10 Ω cm) which can be attributed to electrons generated by oxygen vacancies (intrinsic doping) as demonstrated in our work [5,11]. This value of resistivity is comparable to the as-grown intrinsically doped Ta:TiO_2 films deposited by PLD technique [22,23]. This result is crucial because usually semiconducting TiO_2 film doped with oxygen vacancies turn into highly conducting and transparent polycrystalline anatase film after a post growth annealing (conventional and/or ultra-fast) when combined with the extrinsic dopants (Nb, Ta etc.) as reported in literature [5,22–24]. Post-deposition annealing in argon was performed to activate Nb in TiO_2 lattice and to ionize the oxygen vacancies (see Table 2 for detail). The high resistivity value of 3.8×10^{-1} Ω cm ($\mu_H \sim 7.6$ $cm^2V^{-1}s^{-1}$ and $n_e \sim 1.54 \times 10^{18}$ cm^{-3}) of the films prepared at 4 W (Nb~1.92 at%) is solely attributed to the growth of rutile phase during the film growth and annealing process. The resistivity decreased significantly by two orders of magnitude to 4.11×10^{-3} Ω cm ($\mu_H \sim 0.705$ $cm^2V^{-1}s^{-1}$ and $n_e \sim 2.15 \times 10^{21}$ cm^{-3}) probability due to large amount of dopants and the suppression of rutile structure. The lowest resistivity value obtained for this series of samples is 2.37×10^{-3} Ω cm ($\mu_H \sim 0.596$ $cm^2V^{-1}s^{-1}$ and $n_e \sim 4.43 \times 10^{21}$ cm^{-3}) for TiO_2 films doped with 13.1 at% Nb, which corresponds to a sheet resistance of 158 Ω/sq. The minimum resistivity obtained in this work is slightly higher than that reported for polycrystalline Nb:TiO_2 films (resistivity ~1.4×10^{-3} Ωcm) [5] and intrinsic-extrinsic co-doped Ta:TiO_2 films (resistivity~5×10^{-4} Ωcm) [24]. Interestingly, the resistivity of the films increased again to 1.2×10^{-2} Ω cm ($\mu_H \sim 0.153$ $cm^2V^{-1}s^{-1}$ and $n_e \sim 2.63 \times 10^{21}$ cm^{-3}) for higher Nb concentration (16.0 at%). This five-fold increase in resistivity value could be attributed to the formation of high-resistive rutile phase after the heat treatment in line with the XRD results. The electrical transport properties of the un-doped TiO_2 films do not change significantly with annealing probably due to the film rutile structure. It is important to point out that beside Nb, tantalum (Ta) is also used to modify the electrical and optical properties of TiO_2 films for transparent electrodes applications [22–25]. Using Ta:TiO_2 systems, Mazzolini et al. reported highly transparent (> 80%) and conductive (ρ ~ 5×10^{-4} Ω cm) films with high electron motilities (~11.5–13.0 $cm^2V^{-1}s^{-1}$) for PLD grown films. These findings are significant because considering the wide ranging application of TCOs, it is necessary to expend the dopants range to other dopants like Ta etc.

To elucidate more the relationship between the film structure and their resistivity, we plot the resistivity of the annealed films as a function of the anatase phase proportion in anatase-rutile mixture (see Fig. 5). It is evident from the Figure that the dopants (oxygen vacancies and Nb^{+5}) are more efficient in the anatase phase than the rutile. In other words, the doped films have high resistivity when it contains rutile as a primary or secondary phase. The lowest resistivity of the doped anatase films is probably due to their substantially lower conduction band electron effective mass ($m^* \sim 1$ m_e) compared with rutile ($m^* \sim 8$–20 m_e) [26]. Due to the lower m^*, the carrier mobility ($\mu_H = e\tau/m^*$) in anatase structure is larger than rutile thus favoring the conductivity of the films. Secondly in anatase lattice, the TiO_6 octahedra are predominantly edge-sharing configuration and form spiral channels through the structure for easy electron transport. In contrast in rutile structure, TiO_6 octahedra are mostly located at corner sharing sites, making it unfavorable for charge carrier transport [27]. Therefore, the rutile formation suppresses the carrier transport while the anatase structure facilitates the charge mobility in Nb:TiO_2 system [15]. Furthermore, the critical donor density (n_{dc}) at which the Mott transition take place, bears the relation with the Bohr radius (a_H^*) of the hydrogen-like donor state [4]: $n_{dc} \sim (0.25/a_H^*)^3$. The Bohr radius of anatase-TiO_2 is ~15 Å as compared to 2.6 Å of rutile TiO_2 [4]. Consequently, anatase-TiO_2 exhibits lower critical donor density (5×10^{18} cm^{-3})

Table 2
Nb concentration, film thickness, resistivity (ρ), carrier concentration (n_e), Hall mobility (μ_H) and sheet resistance (R_s) values of the annealed TNO films deposited on glass substrate at 200 °C as a function of different power applied at Nb_2O_5 target.

Power (W)	Nb at%	Thickness (nm)	n_e (cm^{-3})	μ_H ($cm^2V^{-1}s^{-1}$)	ρ (Ω cm)	R_s (Ω/sq.)
0	....	133.1 ± 4.79	.....	....	7.37×10^{-1}	4.91×10^4
4	1.9	170.3 ± 11.44	1.54×10^{18}	7.69	3.8×10^{-1}	2.55×10^4
6	4.9	151.5 ± 9.92	2.15×10^{21}	0.705	4.11×10^{-3}	274
8	9.4	125.8 ± 12.58	3.34×10^{21}	0.763	2.45×10^{-3}	163
10	13.1	151.6 ± 9.98	4.43×10^{21}	0.596	2.37×10^{-3}	158
12	16.0	162.7 ± 7.92	2.63×10^{21}	0.153	1.54×10^{-2}	10^3

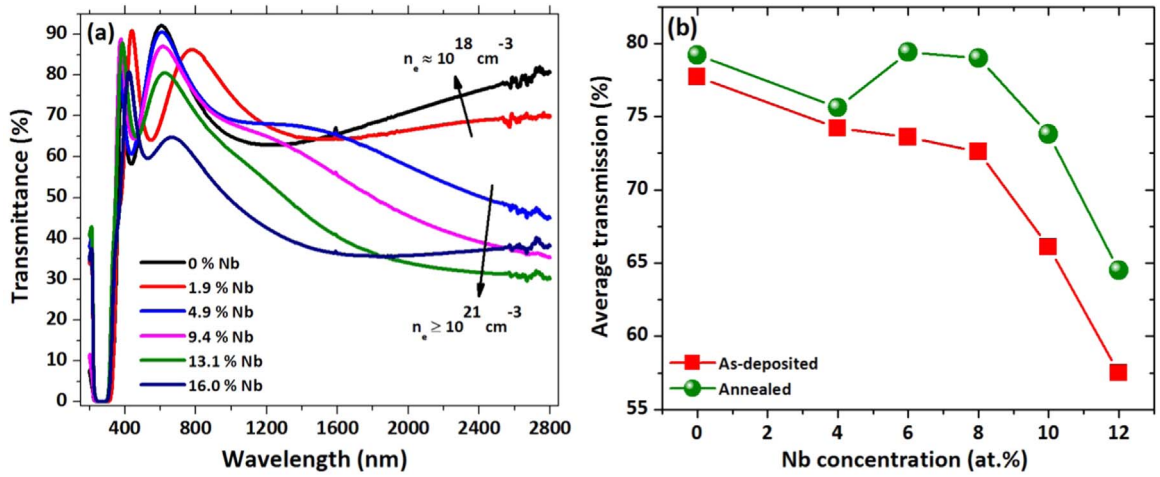

Fig. 6. (a) The transmittance spectra of the annealed films for different Nb amount (b) Comparison of the average visible transmittance of the as-grown (T_{sub} = 200 °C) and annealed films (T_{Ann} = 400 °C) for various Nb amounts.

than rutile (~10^{21} cm^{-3}). This implies that anatase phase is expected to show an insulator-metal transition at lower carrier concentration than rutile making it favored for transparent electrodes application [28]. Further, Lee et al. [7] theoretically demonstrated that Nb-doped anatase TiO_2 has a shallow donor state, delocalized over many Ti sites, forming a shallow defects states. On the other hand, screened exchange predicts a deep state in rutile with the donor electron mainly localized on adjacent Ti sites. Consistent with our observation, Dabnet et al. reported experimentally three orders of magnitude difference in conductivity between the highly crystalline biaxially textured anatase films grown on $SrTiO_3$ and the films on fused silica, which show single phase rutile structure [26]. Similarly, Zhang et al. also found that the rutile phase of Nb:TiO_2 shows much higher resistivity (2–3 orders higher room temperature resistivity) than that of the anatase phase and a considerably lower electrons mobility [4]. From this discussion it is clear that anatase phase of TiO_2 is promising for its transparent conducting properties than rutile structure, which can be controlled by controlling the energetic conditions at the substrates

3.4. Optical properties of Nb:TiO_2 films

Fig. 6(a) illustrates the optical transmittance spectrum of the annealed TNO films in the wavelength range 200–2800 nm. The films were 60–80% transparent in the visible region of the electromagnetic spectrum. It is important to mention here that post-growth annealing in argon enhanced the average visible transmittance by 6–7% compared with their as-grown counterpart (see Fig. 6(b)). The increased in transmittance after thermal annealing could be due to the ionization of oxygen vacancies and densification of the films [15]. The TNO films which showed the best electrical properties ($\rho = 2.73 \times 10^{-3}$ Ω cm) is 75% transparent in the visible region. Notably, due to high carrier density ($> 10^{21}$ cm^{-3}), the films displayed a low transmittance in the NIR region which is ascribed to the absorption due to plasma oscillations of the free conduction band electrons (according to the Drude model), a well-known phenomenon in highly degenerate TCOs films.

The optical gap (E_{OPT}) of the films was evaluated using Tauc model. All the as-grown films exhibited E_{OPT} value 3.18–3.24 eV which is in good agreement with the value reported for the TiO_2 thin films [29]. Generally the E_{OPT} of the as-grown films increased with annealing treatment. For the most conductive film, the E_{OPT} increased from 3.21 to 3.50 eV with thermal annealing. This widening of the optical band gap is attributed to the well-known Burstein-Moss effect, in which the lowest states in the conduction band were blocked and the transition can only take place to energies higher than the Fermi energy [24]. The blue shift in the absorption edge further suggests that doped Nb^{+5} ions act as the dopant in TiO_2. Castro et al. estimated an increment in the band gap of TNO films by ~0.25 eV compared with the bulk anatase (3.20 eV) [30]. Zhang et al. also have found an increase in the band-gap from 3.22 eV for TiO_2 to 3.37 eV for 5% Nb-doped TiO_2 film [4].

Under the application point of view, the prepared films exhibited sheet resistance in the range 158–168 Ω/sq. with transmissivity greater than 85% at 550 nm, which meets the requirement for flat panel displays and touch screen applications. It can also fulfill the need of functional glasses such as electrochromic and low-emissivity glass windows.

4. Conclusion

In conclusion, TiO_2 thin films with various levels of Nb incorporation were grown by RF sputtering at 200 °C and then annealed at 400 °C. It was found that the growth temperature is the key factor influencing the structure, hence the electrical resistivity of the prepared films. The formation of rutile phase has an adverse effect on the conductivity of the films which almost hide the effect of Nb doping on the resistivity of most of the TiO_2 films. It was found that films deposited at substrate temperature of 200 °C and subsequently annealed at 400 °C have mixed anatase and rutile phase, while anatase phase was grown by depositing the films on a cold substrate and then annealed at 350 °C. Under the electrical point of view, the resistivities of the doped films decreased from 3.8×10^{-1} to 4.1×10^{-3} Ω cm when the amounts of anatase in anatase-rutile phases mixture decrease from 52.8% to 32%. Further, the lowest resistivity obtained was around 2.37×10^{-3} Ω cm for the doped TiO_2 films having single phase anatase structure. Our result indicates that the conductivity of the doped films is strongly correlated with the crystalline structure particularly on the amount of anatase phase with respect to rutile. The formation of rutile phase can be controlled by controlling energetic conditions at the substrates.

References

[1] A. Stadler, Transparent conducting oxides—an up-to-date overview, Materials 5 (4) (2012) 661–683.
[2] Y. Furubayashi, T. Hitosugi, Y. Yamamoto, K. Inaba, G. Kinoda, Y. Hirose, T. Shimada, T. Hasegawa, A transparent metal: Nb-doped anatase TiO_2, Appl. Phys. Lett. 86 (25) (2005) 252101.
[3] T. Hitosugi, N. Yamada, S. Nakao, Y. Hirose, T. Hasegawa, Properties of TiO_2-based transparent conducting oxides, Phys. Status Solidi (a) 207 (7) (2010) 1529–1537.
[4] S.X. Zhang, D.C. Kundaliya, W. Yu, S. Dhar, S.Y. Young, L.G. Salamanca-Riba, S.B. Ogale, R.D. Vispute, T. Venkatesan, Niobium doped TiO_2: intrinsic transparent metallic anatase versus highly resistive rutile phase, J. Appl. Phys. 102 (1) (2007) 013701.
[5] K. Safeen, V. Micheli, R. Bartali, G. Gottardi, A. Safeen, H. Ullah, N. Laidani, Synthesis of conductive and transparent Nb-doped TiO2 films: role of the target

material and sputtering gas composition, Mater. Sci. Semicond. Process. 66 (2017) 74–80.
[6] K. Safeen, V. Micheli, R. Bartali, G. Gottardi, N. Laidani, Low temperature growth study of nano-crystalline TiO_2 thin films deposited by RF sputtering, J. Phys. D: Appl. Phys. 48 (29) (2015) 295201.
[7] H.-Y. Lee, J. Robertson, Doping and compensation in Nb-doped anatase and rutile TiO2, J. Appl. Phys. 113 (21) (2013) 213706.
[8] J. Tao, H. Pan, L.M. Wong, T.I. Wong, J. Chai, J. Pan, S. Wang, Mechanism of insulator-to-metal transition in heavily Nb doped anatase TiO_2, Mater. Res. Express 1 (1) (2014) 015911.
[9] H. Nogawa, A. Chikamatsu, Y. Hirose, S. Nakao, H. Kumigashira, M. Oshima, T. Hasegawa, Carrier compensation mechanism in heavily Nb-doped anatase Ti 1 − x Nb x O 2 + δ epitaxial thin films, J. Phys. D: Appl. Phys. 44 (36) (2011) 365404.
[10] M.A. Gillispie, M.F. van Hest, M.S. Dabney, J.D. Perkins, D.S. Ginley, rf magnetron sputter deposition of transparent conducting Nb-doped Ti O_2 films on Sr Ti O_3, J. Appl. Phys. 101 (3) (2007) 033125.
[11] M.K. Safeen, Growth Study and Characterization of TiO_2 Based Thin Films for Low Temperature Synthesis of Transparent Conductive Films, University of Trento, 2016.
[12] R. Bartali, V. Micheli, G. Gottardi, A. Vaccari, M.K. Safeen, N. Laidani, Nano-hardness estimation by means of Ar+ ion etching, Thin Solid Films 589 (2015) 376–380.
[13] R.C. Giorgio Speranza, RxpsG Free Software for XPS Data Processing, Fondazione Bruno Kessler, Trento, 2016.
[14] I. Luciu, R. Bartali, N. Laidani, Influence of hydrogen addition to an Ar plasma on the structural properties of TiO_2 − xthin films deposited by RF sputtering, J. Phys. D: Appl. Phys. 45 (34) (2012) 345302.
[15] N. Laidani, P. Cheyssac, J. Perrière, R. Bartali, G. Gottardi, I. Luciu, V. Micheli, Intrinsic defects and their influence on the chemical and optical properties of TiO_2 − xfilms, J. Phys. D: Appl. Phys. 43 (48) (2010) 485402.
[16] A.N. Banerjee, S.W. Joo, B.-K. Min, Nanocrystalline ZnO thin film deposition on flexible substrate by low-temperature sputtering process for plastic displays, J. Nanosci. Nanotechnol. 14 (10) (2014) 7970–7975.
[17] L. Trotochaud, S.W. Boettcher, Synthesis of rutile-phase Sn x Ti1–x O_2 solid-solution and (SnO2) x/(TiO2) 1–x core/shell nanoparticles with tunable lattice constants and controlled morphologies, Chem. Mater. 23 (22) (2011) 4920–4930.
[18] V. Etacheri, M.K. Seery, S.J. Hinder, S.C. Pillai, Oxygen rich titania: a dopant free, high temperature stable, and visible-light active anatase photocatalyst, Adv. Funct. Mater. 21 (19) (2011) 3744–3752.
[19] W.H. Shah, K. Safeen, G. Rehman, Effects of divalent alkaline earth ions on the magnetic and transport features of La 0.65 A 0.35 Mn 0.95 Fe 0.05 O 3 (A = Ca, Sr, Pb, Ba) compounds, Curr. Appl. Phys. 12 (3) (2012) 742–747.
[20] T. Ishida, M. Okada, T. Tsuchiya, T. Murakami, M. Nakano, Structural and surface property study of sputter deposited transparent conductive Nb-doped titanium oxide films, Thin Solid Films 519 (6) (2011) 1934–1942.
[21] W.-C. Lee, H.-L. Wang, M.-S. Wong, Phase transformation and structures of pure and carbon containing titania thin films annealed in air and in hydrogen, Thin Solid Films 528 (2013) 2–9.
[22] P. Mazzolini, T. Acartürk, D. Chrastina, U. Starke, C.S. Casari, G. Gregori, A.L. Bassi, Controlling the electrical properties of undoped and ta-doped TiO_2 polycrystalline films via ultra-fast-annealing treatments, Adv. Electron. Mater. 2 (3) (2016).
[23] H. Krysova, P. Mazzolini, C.S. Casari, V. Russo, A.L. Bassi, L. Kavan, Electrochemical properties of transparent conducting films of tantalum-doped titanium dioxide, Electrochim. Acta 232 (2017) 44–53.
[24] P. Mazzolini, P. Gondoni, V. Russo, D. Chrastina, C.S. Casari, A.L. Bassi, Tuning of electrical and optical properties of highly conducting and transparent Ta-doped TiO_2 polycrystalline films, J. Phys. Chem. C 119 (13) (2015) 6988–6997.
[25] P. Mazzolini, V. Russo, C. Casari, T. Hitosugi, S. Nakao, T. Hasegawa, A. Li Bassi, Vibrational–electrical properties relationship in donor-doped TiO2 by Raman spectroscopy, J. Phys. Chem. C 120 (33) (2016) 18878–18886.
[26] M.S. Dabney, M.F. van Hest, C.W. Teplin, S.P. Arenkiel, J.D. Perkins, D.S. Ginley, Pulsed laser deposited Nb doped TiO_2 as a transparent conducting oxide, Thin Solid Films 516 (12) (2008) 4133–4138.
[27] K.-H. Hung, P.-W. Lee, W.-C. Hsu, H.C. Hsing, H.-T. Chang, M.-S. Wong, Transparent conducting oxide films of heavily Nb-doped titania by reactive co-sputtering, J. Alloy. Compd. 509 (42) (2011) 10190–10194.
[28] J.-H. Park, S.J. Kang, S.-I. Na, H.H. Lee, S.-W. Kim, H. Hosono, H.-K. Kim, Indium-free, acid-resistant anatase Nb-doped TiO_2 electrodes activated by rapid-thermal annealing for cost-effective organic photovoltaics, Sol. Energy Mater. Sol. Cells 95 (8) (2011) 2178–2185.
[29] P.B. Nair, V.B. Justinvictor, G.P. Daniel, K. Joy, K.C. James Raju, D. Devraj Kumar, P.V. Thomas, Optical parameters induced by phase transformation in RF magnetron sputtered TiO_2 nanostructured thin films, Progress. Nat. Sci.: Mater. Int. 24 (3) (2014) 218–225.
[30] M. Castro, L. Rebouta, P. Alpuim, M. Cerqueira, M. Benelmekki, C. Garcia, E. Alves, N. Barradas, E. Xuriguera, C. Tavares, Optimisation of surface treatments of TiO_2: Nb transparent conductive coatings by a post-hot-wire annealing in a reducing H_2 atm, Thin Solid Films 550 (2014) 404–412.